

Topological zero modes and correlation pumping in an engineered Kondo lattice

Zina Lippo,¹ Elizabeth Louis Pereira,² Jose L. Lado,² and Guangze Chen^{3,*}

¹*Department of Physics, University of Helsinki, Finland*

²*Department of Applied Physics, Aalto University, 02150 Espoo, Finland*

³*Department of Microtechnology and Nanoscience,*

Chalmers University of Technology, 41296 Göteborg, Sweden

(Dated: September 27, 2024)

Topological phases of matter provide a flexible platform to engineer unconventional quantum excitations in quantum materials. Beyond single particle topological matter, in systems with strong quantum many-body correlations, many-body effects can be the driving force for non-trivial topology. Here, we propose a one-dimensional engineered Kondo lattice where the emergence of topological excitations is driven by collective many-body Kondo physics. We first show the existence of topological zero modes in this system by solving the interacting model with tensor networks, and demonstrate their robustness against disorder. To unveil the origin of the topological zero modes, we analyze the associated periodic Anderson model showing that it can be mapped to a topological non-Hermitian model, enabling rationalizing the origin of the topological zero modes. We finally show that the topological invariant of the many-body Kondo lattice can be computed with a correlation matrix pumping method directly with the exact quantum many-body wavefunction. Our results provide a strategy to engineer topological Kondo insulators, highlighting quantum magnetism as a driving force in engineering topological matter.

Introduction. The engineering of topological phases of matter [1, 2] has provided a highly successful strategy to create electronic excitations beyond those found in conventional materials, including chiral [3], helical [4] and Majorana states [5]. The robustness of topological excitations to disorder renders them of interest for a variety of applications, ranging from electronics [1, 2, 6], spintronics [7] to topological quantum computing [8]. Topological phases are often challenging to find in naturally occurring materials [9–11], which has motivated a variety of efforts to create them in artificially engineered systems [12–14]. In particular, a variety of strategies can be leveraged to engineer these states, by combining competing orders [5, 15–17], using external driving [18–20], leveraging coupling to the environment [21–23] or engineering many-body interactions [24–26]. Beyond single-particle topological matter [27], the engineering of quantum many-body effects may ultimately allow creating topological states that have no single particle counterpart [28, 29].

Kondo lattices [30] are a paradigmatic platform where many-body effects dictate the interplay between electronic delocalization and magnetic entanglement formation [11, 31–35]. Topological states have been known to appear in topological Kondo insulators [36, 37], where Kondo screening leads to an effectively topological electronic structure for the single-particle excitations [38, 39]. However, conventional mechanisms to create topological Kondo insulators require strong spin-orbit coupling of localized f electrons [36, 37], and potential material candidates remain restricted [40–43]. Thus, finding alternative strategies to engineer topological matter in Kondo systems will enable creating topological excitations by using quantum magnetism as a fundamental driving force.

Here, we propose a design to realize a topological

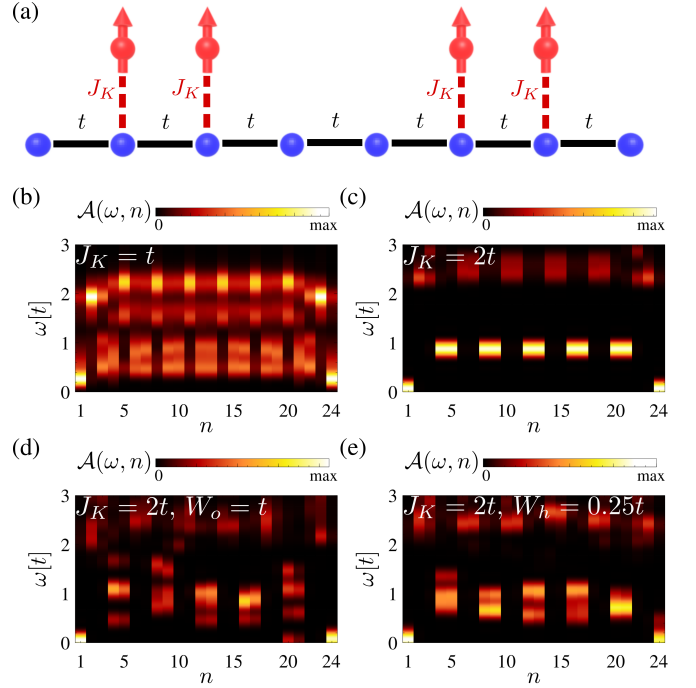


FIG. 1. (a) Schematic of the Kondo lattice model Eq. (1), where the electronic sites (blue) have a uniform hopping t between them. Kondo spins (red) are coupled to some of the electronic sites with strength J_K . Panels (b,c) show the spectral function featuring the zero edge modes. Panels (d,e) show the spectral function for a disordered system, demonstrating the robustness of the zero modes. We took $J_K = t, 2t$ in (b,c) and $J_K = 2t, W_o = t$ and $W_h = 0.25t$ in (d,e).

Kondo insulator in a one-dimensional Kondo lattice, where the topology is solely generated by the many-body Kondo coupling. We first show the existence of zero edge

modes by exactly solving this system with tensor networks and demonstrate their robustness against disorder. We then unveil the topological nature of the edge modes by performing a mapping to a periodic Anderson model, and showing that the topological protection of these zero modes stems from an effective non-Hermitian model. We finally show that the topological invariant can be exactly computed with the many-body wavefunction using a correlation matrix pumping method, that becomes equivalent to the well-known Zak phase for non-interacting systems.

Model and Results. We consider the one-dimensional spin-1/2 Kondo lattice model of the form

$$\mathcal{H} = t \sum_{s,n=1}^{N-1} \left(c_{n+1,s}^\dagger c_{n,s} + h.c. \right) + J_K \sum_{\substack{s,s',\alpha \\ n \in n_K}} c_{n,s}^\dagger \sigma_{ss'}^\alpha c_{n,s'} S_n^\alpha \quad (1)$$

where c_n^\dagger and c_n are electron creation and annihilation operators at site n , $\alpha = x, y, z$, S_n^α is the Kondo spin that is coupled to the electronic site n , $n_K = \{4m+1, 4m+2\} | m \in \mathcal{N}$ is the collection of Kondo sites, and t and J_K are the hopping and Kondo coupling strengths [Fig. 1(a)]. For the sake of concreteness, we consider a chain with 24 fermionic sites and 12 Kondo spin sites. We solve the many-body ground state of the system with a tensor-network formalism. The many-body ground state is a non-magnetic spin singlet state, with all the Kondo spin sites screened by the electronic gas, realizing a minimal example of a non-uniform one-dimensional Kondo screened lattice. The charge excitations of the many-body system can be obtained from the local electronic spectral function

$$\mathcal{A}(\omega, n) = \langle \Omega | c_n \delta(\omega - \mathcal{H} + E_0) c_n^\dagger | \Omega \rangle \quad (2)$$

where $|\Omega\rangle$ is the ground state of the system, E_0 is the ground state energy, and δ is the Dirac delta function. The previous object can be computed with tensor networks using a Chebyshev algorithm [44–47]. As shown in Fig. 1(b)-(c), zero edge modes appear in the chain for non-zero J_K . Due to finite-size effect, these edge modes acquire a finite energy which decreases as J_K increases. This shows that sufficiently large Kondo coupling can induce many-body zero mode excitations at the edge in the Kondo lattice. The appearance of zero edge modes coexists with gapped bulk electronic spectra, as expected from a topological state.

To show that these zero modes are topological, we now demonstrate their robustness against disorder. We consider onsite and hopping disorder taking the form $\mathcal{H}_{\text{onsite}} = \sum_{s,n \neq 1, N} W_o \chi_n c_{n,s}^\dagger c_{n,s}$ and $\mathcal{H}_{\text{hopping}} = \sum_{s,n=1}^{N-1} W_h \chi_n \left(c_{n+1,s}^\dagger c_{n,s} + h.c. \right)$ where W_o, h are the onsite and hopping disorder strength, and χ_n are Gaussian distributed random variables with width 1. We consider $W_o = t$ and $W_h = 0.25t$ in our case. Averaging over 5

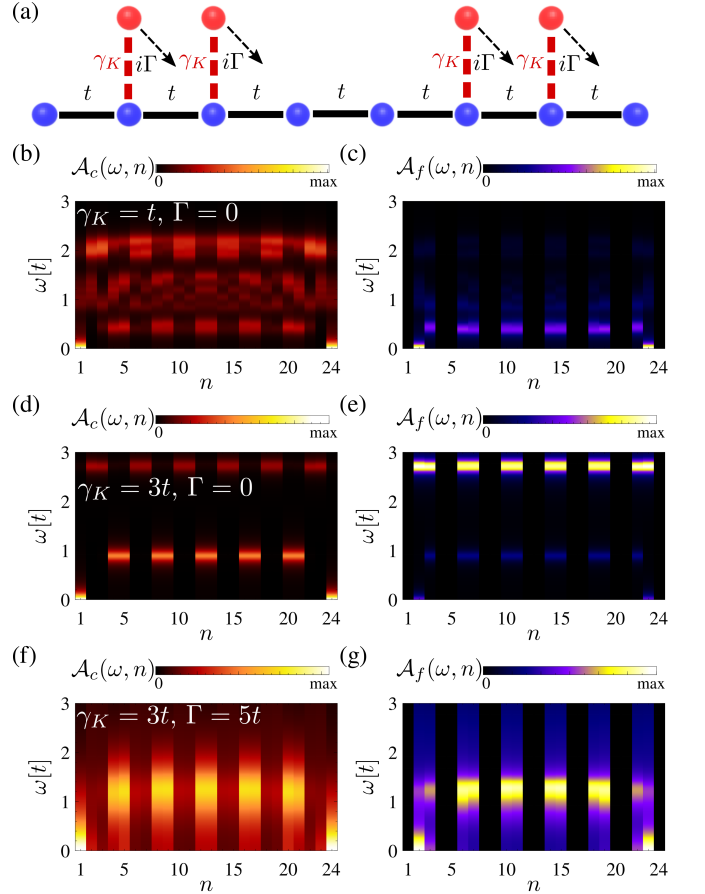


FIG. 2. Spectral function of the effective non-Hermitian Anderson model. (a) The non-Hermitian effective Hamiltonian Eq. (4) stemming from the Dyson equation, where localized fermions (red) are coupled to delocalized sites (blue) with coupling strength γ_K . The spectral functions of the extended (b,d,f) and localized (c,e,g) fermions show the existence of zero modes. We took $\gamma_K = t$ and $\Gamma = 0$ for (b,c), $\gamma_K = 3t$ and $\Gamma = 0$ for (d,e) and $\gamma_K = 3t$ and $\Gamma = 5t$ for (f,g).

different disorder configurations, we obtain Fig. 1(d)-(e), showing that the zero modes are robust against disorder.

Anderson lattice model. To rationalize the origin of the topological zero modes, we note that the Kondo lattice can be understood as stemming from a periodic Anderson model [30] of the form

$$\begin{aligned} H_{\text{PAM}} = & t \sum_{s,n=1}^{N-1} \left(c_{n+1,s}^\dagger c_{n,s} + h.c. \right) \\ & + \gamma_K \sum_{s,n \in n_K} \left(c_{n,s}^\dagger f_{n,s} + h.c. \right) + U \sum_{n \in n_K} f_{n,\uparrow}^\dagger f_{n,\uparrow} f_{n,\downarrow}^\dagger f_{n,\downarrow} \end{aligned} \quad (3)$$

where $f_{n,s}$ is the fermion on Kondo site n with spin s . The localized fermions are coupled to the electrons with coupling strength γ_K , and they have an onsite interaction U . When U is large, this model provides the same physics as the Kondo lattice model. We have neglected

the small dispersion of the localized fermions. We can now obtain an effective model for the delocalized electrons by including the interaction effects through a self-energy stemming from a Dyson equation [48]. Due to the onsite interaction U , the localized fermions acquire a self-energy $\Sigma_f(\omega) = -a_1\omega - i(\Gamma + a_2\omega^2)$ [48] where $a_{1,2}$ and Γ are coefficients. The frequency-dependent terms do not change the qualitative features of the electronic spectrum and are therefore neglected [48]. This results in a finite quasiparticle lifetime $\tau = 1/\Gamma$, and the inverse lifetime Γ in general increases with temperature. With this treatment, we obtain an effective Hamiltonian for Eq. (3) [Fig. 2(a)]:

$$H_{\text{eff}} = t \sum_{s,n=1}^{N-1} \left(c_{n+1,s}^\dagger c_{n,s} + h.c. \right) + \gamma_K \sum_{s,n \in n_K} \left(c_{n,s}^\dagger f_{n,s} + h.c. \right) - i\Gamma \sum_{s,n \in n_K} f_{n,s}^\dagger f_{n,s} \quad (4)$$

To see the distribution of the zero modes after the hybridization, we compute the spectral function of the extended and localized fermions for H_{eff} at different γ_K [Fig. 2(b)-(g)]. The spectral functions are defined as $\mathcal{A}_c(\omega, n) = \langle n | \delta(\omega - H_{\text{eff}}) | n \rangle$ and $\mathcal{A}_f(\omega, n) = \langle n_f | \delta(\omega - H_{\text{eff}}) | n_f \rangle$ where $|n\rangle$ is the local electronic basis at site n and $|n_f\rangle$ is the localized fermion basis coupled to site n . We first consider the case $\Gamma = 0$, i.e. the localized fermions have infinite lifetime. The zero edge modes appear for $\gamma_K > 0$, with both extended and localized fermionic distributions [Fig. 2(b)-(e)]. The ratio between the extended and localized fermionic parts of the zero modes depends on γ_K : the larger γ_K is, the more distribution the zero modes have on the extended fermionic parts. Let us move on to consider $\Gamma > 0$, i.e. the localized fermions have a finite lifetime, where we focus on $\gamma_K = 3t$ regime and see how the finite lifetime influences the topological zero modes. Interestingly, the zero edge modes persist, and they have a lifetime much longer than $1/\Gamma$ [Fig. 2(f)-(g)]. This shows the robustness of the topological zero modes against finite localized fermion lifetime.

The origin of the topological zero modes in Fig. 2 can be further clarified by integrating out the interacting localized modes. This is done by separating the effective Hamiltonian H_{eff} into two parts H_1, H_2 with coupling $H_{12} + H_{12}^\dagger$, and tracing out the part H_2 to obtain an effective Hamiltonian $\mathcal{H}_{\text{eff}}(\omega) = H_1 + \Sigma_e(\omega)$ where $\Sigma_e(\omega) = H_{12}^\dagger(\omega - H_2)^{-1}H_{12}$ is the frequency-dependent self-energy. We first consider the following separation of the Hamiltonian (Fig. 3(a)): the non-Kondo coupled sites $H_1 = t \sum_{s,n=1}^{N/4-1} c_{4n+1,s}^\dagger c_{4n,s} + h.c.$, the Kondo coupled sites $H_2 = t \sum_{s,n=1}^{N/4-1} \left(c_{4n-2,s}^\dagger c_{4n-1,s} + h.c. \right) + \gamma_K \sum_{s,n \in n_K} \left(c_{n,s}^\dagger f_{n,s} + h.c. \right) - i\Gamma \sum_{s,n \in n_K} f_{n,s}^\dagger f_{n,s}$, and the coupling between both $H_{12} =$

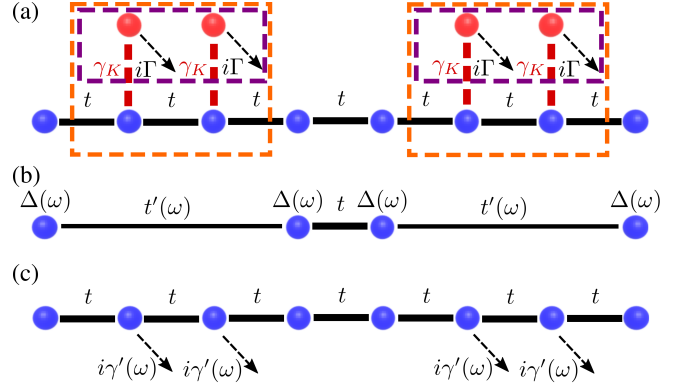


FIG. 3. Schematic of the strategies to derive the effective Hamiltonian. Panel (a) shows two ways to separate the effective Hamiltonian Eq. (4) (dashed orange and purple rectangles). Panel (b) shows the effective Hamiltonian obtained from the dashed orange separation in panel (a). This model has a frequency-dependent hopping $t'(\omega)$ and a uniform onsite loss $\Delta(\omega)$, given below Eq. (5). At $\omega = 0$, it reduces to an SSH model with $|t'| = t$, which is known to host topological zero modes. Panel (c) shows the effective Hamiltonian obtained from the dashed purple separation in panel (a). This model has a frequency-dependent onsite loss $i\gamma'(\omega)$ given below Eq. (6). At $\omega = 0$, it reduces to a model with non-Hermitian topological zero edge modes.

$t \sum_{s,n=1}^{N/4-1} \left(c_{4n-2,s}^\dagger c_{4n-3,s} + c_{4n-1,s}^\dagger c_{4n,s} \right)$. The effective Hamiltonian is then given by [49]: [Fig. 3(b)]

$$\mathcal{H}_{\text{eff}}^{\text{SSH}} = t \sum_{s,n=1}^{N/4-1} \left(c_{4n+1,s}^\dagger c_{4n,s} + h.c. \right) + t'(\omega) \sum_{s,n=0}^{N/4-1} \left(c_{4n+4,s}^\dagger c_{4n+1,s} + h.c. \right) + \Delta(\omega) \sum_{s,n=0}^{N/4-1} \left(c_{4n+1,s}^\dagger c_{4n+1,s} + c_{4n+4,s}^\dagger c_{4n+4,s} \right) \quad (5)$$

where $t'(\omega) = -t \frac{(\omega+i\Gamma)^2 t^2}{(\omega+i\Gamma)^2 t^2 - [\omega(\omega+i\Gamma) - \gamma_K^2]^2}$ and $\Delta(\omega) = -\frac{(\omega+i\Gamma)t^2[\omega(\omega+i\Gamma) - \gamma_K^2]}{(\omega+i\Gamma)^2 t^2 - [\omega(\omega+i\Gamma) - \gamma_K^2]^2}$. In particular, at $\omega = 0$, $t'(0) = -t \frac{\Gamma^2 t^2}{\Gamma^2 t^2 + \gamma_K^4}$ and $\Delta(0) = -it \frac{\Gamma t \gamma_K^2}{\Gamma^2 t^2 + \gamma_K^4}$, and the effective Hamiltonian Eq. (5) reduces to a topologically non-trivial Su-Schrieffer-Heeger (SSH) model with $|t'(0)| < t$ and a uniform onsite loss $\Delta(0)$.

Beyond the topological origin based on the associated SSH model, the presence of loss motivates understanding the zero modes directly from the non-Hermitian topology of the effective model. This is obtained by the following separation of H_{eff} , shown in Fig. 3(a): the delocalized sites $H_1 = t \sum_{s,n=1}^{N-1} \left(c_{n+1,s}^\dagger c_{n,s} + h.c. \right)$, the localized sites $H_2 = -i\Gamma \sum_{s,n \in n_K} f_{n,s}^\dagger f_{n,s}$, and the interaction be-

tween them $H_{12} = \gamma_K \sum_{s,n \in n_K} c_{n,s} f_{n,s}^\dagger$. The effective Hamiltonian in this case is given by: [Fig. 3(c)]

$$\mathcal{H}_{\text{eff}}^{\text{NH}} = t \sum_{s,n=1}^{N-1} \left(c_{n+1,s}^\dagger c_{n,s} + h.c. \right) + i\gamma'_\omega \sum_{s,n \in n_K} c_{n,s}^\dagger c_{n,s} \quad (6)$$

where $\gamma'_\omega = -\frac{\gamma_K^2}{\Gamma - i\omega}$. At $\omega = 0$, this model reduces to a non-Hermitian model known to be topological with zero modes for $\gamma_K^2/\Gamma \neq 0$ [50–52]. Thus, for $\Gamma \neq 0$, the effective non-Hermitian model provides an alternative understanding of the topological zero modes.

Many-body topological invariant. The above analysis identifies the topological origin of the zero modes in the effective Hamiltonian Eq. (4). To be more concrete on the topological nature of the many-body zero modes, we introduce a correlation matrix pumping method to compute the many-body topological invariant of the Kondo lattice Eq. (1). For a unit cell with twisted boundary conditions, the twist-dependent Hamiltonian is given by

$$\begin{aligned} \mathcal{H}^{\text{pump}}(\phi) = & t \sum_{s,n=1}^{N-1} \left(c_{n+1,s}^\dagger c_{n,s} + h.c. \right) \\ & + \sum_s \left(e^{i\phi} c_{N,s}^\dagger c_{1,s} + h.c. \right) \quad (7) \\ & + J_K \sum_{\substack{s,s',\alpha \\ n \in n_K}} c_{n,s}^\dagger \sigma_{ss'}^\alpha c_{n,s'} S_n^\alpha \end{aligned}$$

The Hamiltonian has a twist-dependent ground state $|\Omega_\phi\rangle$, allowing us to define the correlation matrix [53–56] as

$$\Xi_{is,js'}(\phi) = \langle \Omega_\phi | c_{is}^\dagger c_{js'} | \Omega_\phi \rangle. \quad (8)$$

This correlation matrix features eigenvectors $\Xi|v_\phi\rangle = \chi_\phi|v_\phi\rangle$, which in the non-interacting case directly correspond to the single particle eigenstates of the Hamiltonian [57, 58]. The eigenvalues χ_ϕ of Ξ are ranged in the interval $[0, 1]$, and in the non-interacting limit non-occupied eigenstates have eigenvalue 0 whereas occupied states have eigenvalue 1. In the interacting limit, the eigenvalues χ_ϕ are no longer integer [59–62]. A correlation matrix Ξ featuring a gap in its eigenvalues χ_ϕ can be used to characterize the topology of the many-body ground state. Specifically, the geometric phase of the correlation matrix allows to characterize the topological classification of the ground state, and the classification becomes equivalent to the one stemming from the Bloch Hamiltonian in the non-interacting limit. Since the many-body ground state of the Kondo lattice does not break time-reversal symmetry, we define the spinless correlation matrix as

$$\bar{\Xi}_{ij}(\phi) = \frac{1}{2} \sum_s \langle \Omega_\phi | c_{is}^\dagger c_{js} | \Omega_\phi \rangle. \quad (9)$$

We denote the eigenstates and eigenvalues of $\bar{\Xi}_{ij}(\phi)$ as $\bar{\chi}_\phi$ and $|\bar{v}_\phi\rangle$. The many-body geometric phase is defined as

$$\Phi = i \int_{\phi=0}^{2\pi} \sum_{\bar{\chi}_\phi > \Delta} \langle \bar{v}_\phi | \partial_\phi | \bar{v}_\phi \rangle d\phi, \quad (10)$$

where Δ denotes the location of the spectral gap in the entanglement spectrum that we take as $\Delta = 0.5$ [63]. For a non-interacting spinful dimerized model, the geometric phase Φ is equivalent to the Zak phase of each spin sector $0, \pi$ for the trivial and topological configurations. In the presence of a gap in the correlation spectra, the geometric phase Φ must remain quantized, and as a result, it allows to characterize the topological states of a many-body Hamiltonian such as the Kondo lattice model. Eq. (10) can be directly computed using the many-body ground state computed exactly for the Kondo lattice model with tensor networks, which yields a value $\Phi = \pm\pi$ for any non-zero Kondo coupling $J_K > 0$. It is finally worth noting that the formulation of a topological invariant in terms of the pumping of the correlation matrix can be readily extended to other interacting fermionic states, including interacting Chern insulators, quantum spin hall insulators, and topological crystalline phases.

Finally, let us comment on the experimental realization of our proposal. The one-dimensional electron gas can be realized in van der Waals materials, using twin boundaries in monolayers [64], stacking domain walls bilayers [65] or helical networks in twisted bilayers [66]. The Kondo lattice can be formed by depositing single magnetic atoms with scanning tunneling microscopy (STM), which has allowed to create controllable Kondo systems [67–69], and where the many-body spectral functions is measured through tunneling spectroscopy.

Conclusion. We have shown the emergence of topological zero modes in an engineered one-dimensional Kondo lattice, where the topology is solely driven by Kondo physics. This phenomenology was first demonstrated with an exact solution of the Kondo lattice model with tensor networks, and afterward by mapping the Kondo lattice model to an effective topological non-Hermitian model. Finally, we have introduced a correlation matrix pumping method and showed that it allows us to compute the many-body topological invariant of the Kondo lattice model from the exact wavefunction. Our results put forward the engineering of Kondo lattices as a promising approach to create topological zero modes, enabling the use of quantum magnetism as a driving force to create many-body topological phases of matter.

Acknowledgements We acknowledge the computational resources provided by the Aalto Science-IT project. G.C. is supported by European Union's Horizon 2023 research and innovation programme under the Marie Skłodowska-Curie grant agreement No. 101146565, Z.L., E.L.P., and J.L.L. acknowledge financial support from the Academy of Finland Projects

Nos.331342 and 358088, the Nokia Industrial Doctoral School in Quantum Technology, the Jane and Aatos Erkkö Foundation and the Finnish Quantum Flagship.

* guangze@chalmers.se

- [1] M. Z. Hasan and C. L. Kane, Colloquium: Topological insulators, *Rev. Mod. Phys.* **82**, 3045 (2010).
- [2] X.-L. Qi and S.-C. Zhang, Topological insulators and superconductors, *Rev. Mod. Phys.* **83**, 1057 (2011).
- [3] C.-Z. Chang, C.-X. Liu, and A. H. MacDonald, Colloquium: Quantum anomalous hall effect, *Rev. Mod. Phys.* **95**, 011002 (2023).
- [4] J. Maciejko, T. L. Hughes, and S.-C. Zhang, The quantum spin hall effect, *Annual Review of Condensed Matter Physics* **2**, 31–53 (2011).
- [5] J. Alicea, New directions in the pursuit of majorana fermions in solid state systems, *Reports on Progress in Physics* **75**, 076501 (2012).
- [6] D. Xiao, M.-C. Chang, and Q. Niu, Berry phase effects on electronic properties, *Rev. Mod. Phys.* **82**, 1959 (2010).
- [7] L. Šmejkal, Y. Mokrousov, B. Yan, and A. H. MacDonald, Topological antiferromagnetic spintronics, *Nature Physics* **14**, 242–251 (2018).
- [8] C. Nayak, S. H. Simon, A. Stern, M. Freedman, and S. Das Sarma, Non-abelian anyons and topological quantum computation, *Rev. Mod. Phys.* **80**, 1083 (2008).
- [9] Y. Deng, Y. Yu, M. Z. Shi, Z. Guo, Z. Xu, J. Wang, X. H. Chen, and Y. Zhang, Quantum anomalous hall effect in intrinsic magnetic topological insulator mnbi 2 te 4, *Science* **367**, 895–900 (2020).
- [10] S. Wu, V. Fatemi, Q. D. Gibson, K. Watanabe, T. Taniguchi, R. J. Cava, and P. Jarillo-Herrero, Observation of the quantum spin hall effect up to 100 kelvin in a monolayer crystal, *Science* **359**, 76–79 (2018).
- [11] L. Jiao, S. Howard, S. Ran, Z. Wang, J. O. Rodriguez, M. Sigrist, Z. Wang, N. P. Butch, and V. Madhavan, Chiral superconductivity in heavy-fermion metal uTe₂, *Nature* **579**, 523–527 (2020).
- [12] E. Y. Andrei, D. K. Efetov, P. Jarillo-Herrero, A. H. MacDonald, K. F. Mak, T. Senthil, E. Tutuc, A. Yazdani, and A. F. Young, The marvels of moiré materials, *Nature Reviews Materials* **6**, 201–206 (2021).
- [13] D.-J. Choi, N. Lorente, J. Wiebe, K. von Bergmann, A. F. Otte, and A. J. Heinrich, Colloquium: Atomic spin chains on surfaces, *Rev. Mod. Phys.* **91**, 041001 (2019).
- [14] T. Ozawa, H. M. Price, A. Amo, N. Goldman, M. Hafezi, L. Lu, M. C. Rechtsman, D. Schuster, J. Simon, O. Zeitlinger, and I. Carusotto, Topological photonics, *Rev. Mod. Phys.* **91**, 015006 (2019).
- [15] T. Dvir, G. Wang, N. van Looy, C.-X. Liu, G. P. Mazur, A. Bordin, S. L. D. Ten Haaf, J.-Y. Wang, D. van Driel, F. Zlati, X. Li, F. K. Malinowski, S. Gazibegovic, G. Badawy, E. P. A. M. Bakkers, M. Wimmer, and L. P. Kouwenhoven, Realization of a minimal kitaev chain in coupled quantum dots, *Nature* **614**, 445–450 (2023).
- [16] S. Kezilebieke, M. N. Huda, V. Vaño, M. Aapro, S. C. Ganguli, O. J. Silveira, S. Głodzik, A. S. Foster, T. Ojanen, and P. Liljeroth, Topological superconductivity in a van der waals heterostructure, *Nature* **588**, 424–428 (2020).
- [17] L. Schneider, P. Beck, J. Neuhaus-Steinmetz, L. Rózsa, T. Posske, J. Wiebe, and R. Wiesendanger, Precursors of majorana modes and their length-dependent energy oscillations probed at both ends of atomic shiba chains, *Nature Nanotechnology* **17**, 384–389 (2022).
- [18] G. Jotzu, M. Messer, R. Desbuquois, M. Lebrat, T. Uehlinger, D. Greif, and T. Esslinger, Experimental realization of the topological haldane model with ultracold fermions, *Nature* **515**, 237–240 (2014).
- [19] J. W. McIver, B. Schulte, F.-U. Stein, T. Matsuyama, G. Jotzu, G. Meier, and A. Cavalleri, Light-induced anomalous hall effect in graphene, *Nature Physics* **16**, 38–41 (2019).
- [20] M. S. Rudner and N. H. Lindner, Band structure engineering and non-equilibrium dynamics in floquet topological insulators, *Nature Reviews Physics* **2**, 229–244 (2020).
- [21] E. J. Bergholtz, J. C. Budich, and F. K. Kunst, Exceptional topology of non-hermitian systems, *Rev. Mod. Phys.* **93**, 015005 (2021).
- [22] T. Dai, Y. Ao, J. Mao, Y. Yang, Y. Zheng, C. Zhai, Y. Li, J. Yuan, B. Tang, Z. Li, J. Luo, W. Wang, X. Hu, Q. Gong, and J. Wang, Non-hermitian topological phase transitions controlled by nonlinearity, *Nature Physics* **20**, 101–108 (2023).
- [23] G. Harari, M. A. Bandres, Y. Lumer, M. C. Rechtsman, Y. D. Chong, M. Khajavikhan, D. N. Christodoulides, and M. Segev, Topological insulator laser: Theory, *Science* **359**, 10.1126/science.aar4003 (2018).
- [24] M. Rösner and J. L. Lado, Inducing a many-body topological state of matter through coulomb-engineered local interactions, *Phys. Rev. Res.* **3**, 013265 (2021).
- [25] X. Liu, Z. Wang, K. Watanabe, T. Taniguchi, O. Vafek, and J. I. A. Li, Tuning electron correlation in magic-angle twisted bilayer graphene using coulomb screening, *Science* **371**, 1261–1265 (2021).
- [26] M. Serlin, C. L. Tschirhart, H. Polshyn, Y. Zhang, J. Zhu, K. Watanabe, T. Taniguchi, L. Balents, and A. F. Young, Intrinsic quantized anomalous hall effect in a moiré heterostructure, *Science* **367**, 900–903 (2020).
- [27] T. Senthil, Symmetry-protected topological phases of quantum matter, *Annual Review of Condensed Matter Physics* **6**, 299 (2015).
- [28] Y. Zeng, Z. Xia, K. Kang, J. Zhu, P. Knüppel, C. Vaswani, K. Watanabe, T. Taniguchi, K. F. Mak, and J. Shan, Thermodynamic evidence of fractional chern insulator in moiré mote₂, *Nature* **622**, 69–73 (2023).
- [29] Z. Lu, T. Han, Y. Yao, A. P. Reddy, J. Yang, J. Seo, K. Watanabe, T. Taniguchi, L. Fu, and L. Ju, Fractional quantum anomalous hall effect in multilayer graphene, *Nature* **626**, 759–764 (2024).
- [30] H. Tsunetsugu, M. Sigrist, and K. Ueda, The ground-state phase diagram of the one-dimensional kondo lattice model, *Rev. Mod. Phys.* **69**, 809 (1997).
- [31] G. R. Stewart, Heavy-fermion systems, *Rev. Mod. Phys.* **56**, 755 (1984).
- [32] A. Yazdani, E. H. da Silva Neto, and P. Aynajian, Spectroscopic imaging of strongly correlated electronic states, *Annu. Rev. Condens. Matter Phys.* **7**, 11 (2016).
- [33] M. Dzero, J. Xia, V. Galitski, and P. Coleman, Topological Kondo insulators, *Annu. Rev. Condens. Matter Phys.* **7**, 249 (2016).
- [34] S. Wirth and F. Steglich, Exploring heavy fermions from macroscopic to microscopic length scales, *Nat. Rev.*

- Mater.* **1**, 16051 (2016).
- [35] V. Vaño, M. Amini, S. C. Ganguli, G. Chen, J. L. Lado, S. Kezilebieke, and P. Liljeroth, Artificial heavy fermions in a van der waals heterostructure, *Nature* **599**, 582–586 (2021).
- [36] M. Dzero, J. Xia, V. Galitski, and P. Coleman, Topological kondo insulators, *Annual Review of Condensed Matter Physics* **7**, 249–280 (2016).
- [37] M. Dzero, K. Sun, V. Galitski, and P. Coleman, Topological kondo insulators, *Phys. Rev. Lett.* **104**, 106408 (2010).
- [38] M. Neupane, N. Alidoust, S.-Y. Xu, T. Kondo, Y. Ishida, D. J. Kim, C. Liu, I. Belopolski, Y. J. Jo, T.-R. Chang, H.-T. Jeng, T. Durakiewicz, L. Balicas, H. Lin, A. Bansil, S. Shin, Z. Fisk, and M. Z. Hasan, Surface electronic structure of the topological kondo-insulator candidate correlated electron system smb6, *Nature Communications* **4**, 10.1038/ncomms3991 (2013).
- [39] N. Xu, P. K. Biswas, J. H. Dil, R. S. Dhaka, G. Landolt, S. Muff, C. E. Matt, X. Shi, N. C. Plumb, M. Radović, E. Pomjakushina, K. Conder, A. Amato, S. V. Borisenko, R. Yu, H.-M. Weng, Z. Fang, X. Dai, J. Mesot, H. Ding, and M. Shi, Direct observation of the spin texture in smb6 as evidence of the topological kondo insulator, *Nature Communications* **5**, 10.1038/ncomms5566 (2014).
- [40] K.-J. Xu, S.-D. Chen, Y. He, J. He, S. Tang, C. Jia, E. Yue Ma, S.-K. Mo, D. Lu, M. Hashimoto, T. P. Devereaux, and Z.-X. Shen, Metallic surface states in a correlated d-electron topological kondo insulator candidate f5b2, *Proceedings of the National Academy of Sciences* **117**, 15409–15413 (2020).
- [41] H. Pirie, E. Mascot, C. E. Matt, Y. Liu, P. Chen, M. H. Hamidian, S. Saha, X. Wang, J. Paglione, G. Luke, D. Goldhaber-Gordon, C. F. Hirjibehedin, J. C. S. Davis, D. K. Morr, and J. E. Hoffman, Visualizing the atomic-scale origin of metallic behavior in kondo insulators, *Science* **379**, 1214–1218 (2023).
- [42] H. Pirie, Y. Liu, A. Soumyanarayanan, P. Chen, Y. He, M. M. Yee, P. F. S. Rosa, J. D. Thompson, D.-J. Kim, Z. Fisk, X. Wang, J. Paglione, D. K. Morr, M. H. Hamidian, and J. E. Hoffman, Imaging emergent heavy dirac fermions of a topological kondo insulator, *Nature Physics* **16**, 52–56 (2019).
- [43] D. Guerci, K. P. Lucht, V. Crépel, J. Cano, J. H. Pixley, and A. J. Millis, *Topological kondo semimetal and insulator in ab-stacked heterobilayer transition metal dichalcogenides* (2024), [arXiv:2407.12912 \[cond-mat.str-el\]](https://arxiv.org/abs/2407.12912).
- [44] A. Weiße, G. Wellein, A. Alvermann, and H. Fehske, The kernel polynomial method, *Rev. Mod. Phys.* **78**, 275 (2006).
- [45] J. L. Lado and O. Zilberberg, Topological spin excitations in harper-heisenberg spin chains, *Phys. Rev. Res.* **1**, 033009 (2019).
- [46] M. Fishman, S. R. White, and E. M. Stoudenmire, The ITensor Software Library for Tensor Network Calculations, *SciPost Phys. Codebases* , 4 (2022).
- [47] dmrgpy library, <https://github.com/joselado/dmrgpy>.
- [48] Y. Nagai, Y. Qi, H. Isobe, V. Kozii, and L. Fu, Dmft reveals the non-hermitian topology and fermi arcs in heavy-fermion systems, *Phys. Rev. Lett.* **125**, 227204 (2020).
- [49] See Supplemental Material for details.
- [50] K. Takata and M. Notomi, Photonic topological insulating phase induced solely by gain and loss, *Phys. Rev. Lett.* **121**, 213902 (2018).
- [51] W. Brzezicki and T. Hyart, Hidden chern number in one-dimensional non-hermitian chiral-symmetric systems, *Phys. Rev. B* **100**, 161105 (2019).
- [52] G. Chen, F. Song, and J. L. Lado, Topological spin excitations in non-hermitian spin chains with a generalized kernel polynomial algorithm, *Phys. Rev. Lett.* **130**, 100401 (2023).
- [53] R.-Q. He and Z.-Y. Lu, Quantum renormalization groups based on natural orbitals, *Phys. Rev. B* **89**, 085108 (2014).
- [54] Y. Lu, M. Höppner, O. Gunnarsson, and M. W. Haverkort, Efficient real-frequency solver for dynamical mean-field theory, *Phys. Rev. B* **90**, 085102 (2014).
- [55] M. T. Fishman and S. R. White, Compression of correlation matrices and an efficient method for forming matrix product states of fermionic gaussian states, *Phys. Rev. B* **92**, 075132 (2015).
- [56] F. Aikebaier, T. Ojanen, and J. L. Lado, Machine learning the kondo entanglement cloud from local measurements, *Phys. Rev. B* **109**, 195125 (2024).
- [57] P.-O. Löwdin, Quantum theory of many-particle systems. i. physical interpretations by means of density matrices, natural spin-orbitals, and convergence problems in the method of configurational interaction, *Phys. Rev.* **97**, 1474 (1955).
- [58] P. E. M. Siegbahn, J. Almlöf, A. Heiberg, and B. O. Roos, The complete active space scf (casscf) method in a newton–raphson formulation with application to the hno molecule, *The Journal of Chemical Physics* **74**, 2384–2396 (1981).
- [59] C. Yang and A. E. Feiguin, Unveiling the internal entanglement structure of the kondo singlet, *Phys. Rev. B* **95**, 115106 (2017).
- [60] M. Debertolis, Few-body nature of kondo correlated ground states, in *Quantum Impurity Problems in the Framework of Natural Orbitals* (Springer Nature Switzerland, 2024) p. 39–57.
- [61] T. I. Vanhala and T. Ojanen, Complexity of fermionic states, *Phys. Rev. Res.* **6**, 023178 (2024).
- [62] F. Aikebaier, T. Ojanen, and J. L. Lado, Extracting electronic many-body correlations from local measurements with artificial neural networks, *SciPost Phys. Core* **6**, 030 (2023).
- [63] Δ can be taken as any value inside the correlation gap.
- [64] T. Zhu, W. Ruan, Y.-Q. Wang, H.-Z. Tsai, S. Wang, C. Zhang, T. Wang, F. Liou, K. Watanabe, T. Taniguchi, J. B. Neaton, A. Weber-Bargioni, A. Zettl, Z. Q. Qiu, G. Zhang, F. Wang, J. E. Moore, and M. F. Crommie, Imaging gate-tunable tomonaga–luttinger liquids in 1h-mose2 mirror twin boundaries, *Nature Materials* **21**, 748–753 (2022).
- [65] H. Li, Z. Xiang, T. Wang, M. H. Naik, W. Kim, J. Nie, S. Li, Z. Ge, Z. He, Y. Ou, R. Banerjee, T. Taniguchi, K. Watanabe, S. Tongay, A. Zettl, S. G. Louie, M. P. Zaletel, M. F. Crommie, and F. Wang, Imaging tunable luttinger liquid systems in van der waals heterostructures, *Nature* **631**, 765–770 (2024).
- [66] P. Rickhaus, J. Wallbank, S. Slizovskiy, R. Pisoni, H. Overweg, Y. Lee, M. Eich, M.-H. Liu, K. Watanabe, T. Taniguchi, T. Ihn, and K. Ensslin, Transport through a network of topological channels in twisted bilayer graphene, *Nano Letters* **18**, 6725–6730 (2018).
- [67] H. C. Manoharan, C. P. Lutz, and D. M. Eigler, Quantum mirages formed by coherent projection of electronic

- structure, *Nature* **403**, 512–515 (2000).
- [68] Q. L. Li, C. Zheng, R. Wang, B. F. Miao, R. X. Cao, L. Sun, D. Wu, Y. Z. Wu, S. C. Li, B. G. Wang, and H. F. Ding, Role of the surface state in the kondo resonance width of a co single adatom on ag(111), *Phys. Rev. B* **97**, 035417 (2018).
- [69] M. Aapro, A. Kipnis, J. L. Lado, S. Kezilebieke, and P. Liljeroth, Tuning spinaron and kondo resonances via quantum confinement, *Phys. Rev. B* **109**, 195415 (2024).

Supplemental Material for “Topological zero modes and correlation pumping in an engineered Kondo lattice”

(Dated: September 27, 2024)

EFFECTIVE HAMILTONIAN ANALYSIS

Here we show the effective Hamiltonian analysis for

$$\begin{aligned}
 H_1 &= t \sum_{n=1}^{N/4-1} \sum_s \left(c_{4n+1,s}^\dagger c_{4n,s} + c_{4n,s}^\dagger c_{4n+1,s} \right) \\
 H_2 &= t \sum_{n=1}^{N/4-1} \sum_s \left(c_{4n-2,s}^\dagger c_{4n-3,s} + c_{4n-3,s}^\dagger c_{4n-2,s} \right) \\
 &\quad + \gamma_K \sum_{n \in n_K} \sum_s \left(c_{n,s}^\dagger f_{n,s} + f_{n,s}^\dagger c_{n,s} \right) \\
 &\quad - i\Gamma \sum_{n \in n_K} \sum_s f_{n,s}^\dagger f_{n,s} \\
 H_{12} &= t \sum_{n=1}^{N/4-1} \sum_s \left(c_{4n-2,s}^\dagger c_{4n-3,s} + c_{4n-1,s}^\dagger c_{4n,s} \right).
 \end{aligned} \tag{S1}$$

whose effective Hamiltonian is $H_{\text{eff}}(\omega) = H_1 + \Sigma_e(\omega)$ where $\Sigma_e(\omega) = H_{12}^\dagger(\omega - H_2)^{-1}H_{12}$.

We first note that H_{12} is block-diagonal with a periodicity of 4 sites. Thus, solving the self-energy $\Sigma_e(\omega)$ reduces to solving it in a single unit cell with

$$\begin{aligned}
 H_2 &= t \sum_s \left(c_{2,s}^\dagger c_{3,s} + c_{3,s}^\dagger c_{2,s} \right) \\
 &\quad + \gamma_K \sum_{n=2,3} \sum_s \left(c_{n,s}^\dagger f_{n,s} + f_{n,s}^\dagger c_{n,s} \right) \\
 &\quad - i\Gamma \sum_{n=2,3} \sum_s f_{n,s}^\dagger f_{n,s} \\
 H_{12} &= t \sum_s \left(c_{2,s}^\dagger c_{1,s} + c_{3,s}^\dagger c_{4,s} \right)
 \end{aligned} \tag{S2}$$

In the matrix form:

$$\begin{aligned}
 \omega - H_2 &= \begin{pmatrix} \omega & -t & -\gamma_K & -\gamma_K \\ -t & \omega & & \\ -\gamma_K & & \omega + i\Gamma & \\ & -\gamma_K & & \omega + i\Gamma \end{pmatrix} \\
 H_{12} &= \begin{pmatrix} -t & 0 \\ 0 & -t \\ 0 & 0 \\ 0 & 0 \end{pmatrix}
 \end{aligned} \tag{S3}$$

To get $\Sigma_e(\omega)$, we only need to solve the first two columns of $(\omega - H_2)^{-1}$ due to the form of H_{12} :

$$(\omega - H_2)^{-1} = \begin{pmatrix} a(\omega + i\Gamma) & b(\omega + i\Gamma) & \cdots & \cdots \\ b(\omega + i\Gamma) & a(\omega + i\Gamma) & \cdots & \cdots \\ a\gamma_K & b\gamma_K & \cdots & \cdots \\ b\gamma_K & a\gamma_K & \cdots & \cdots \end{pmatrix} \tag{S4}$$

where

$$a = -\frac{[\omega(\omega + i\Gamma) - \gamma_k^2]}{(\omega + i\Gamma)^2 t^2 - [\omega(\omega + i\Gamma) - \gamma_k^2]^2} \tag{S5}$$

$$b = -\frac{(\omega + i\Gamma)t}{(\omega + i\Gamma)^2 t^2 - [\omega(\omega + i\Gamma) - \gamma_k^2]^2}. \tag{S6}$$

Thus,

$$\Sigma_e(\omega) = \begin{pmatrix} \Delta(\omega) & t'(\omega) \\ t'(\omega) & \Delta(\omega) \end{pmatrix} \tag{S7}$$

with

$$t'(\omega) = a(\omega + i\Gamma)t^2 \tag{S8}$$

$$\Delta(\omega) = b(\omega + i\Gamma)t^2. \tag{S9}$$

This gives rise to the effective model Eq. (7) in the main text.

SPIN ROTATION PUMPING

Here we present an alternative method for computing the topological invariant of our Kondo lattice model via spin rotation pumping. The effective SSH model Eq.(9) motivates the Zak phase, which is 0 and π for a topologically trivial and non-trivial SSH model, as the topological invariant for our Kondo lattice model. However, due to spin-degeneracy, the Zak phase takes a value of 2π when our model is topologically non-trivial. In order to overcome this limitation of the Zak phase, we thus define the topological invariant through a many-body spin rotation pumping that leads to a well defined topological phase of π for a spinful system. This is done by considering the spin-rotational twisted boundary condition:

$$\begin{aligned}
 \mathcal{H}_{\text{spin}}(\phi) &= t \sum_{s,n=1}^{N-1} \left(c_{n+1,s}^\dagger c_{n,s} + h.c. \right) \\
 &\quad + \sum_{s,s'} \left(e^{\frac{i}{2}\phi \vec{\sigma}_{ss'} \cdot \hat{e}} c_{N,s}^\dagger c_{1,s'} + h.c. \right) \\
 &\quad + J_K \sum_{\substack{s,s',\alpha \\ n \in n_K}} c_{n,s}^\dagger \sigma_{ss'}^\alpha c_{n,s'} S_n^\alpha
 \end{aligned} \tag{S10}$$

where \hat{e} denotes the spin rotation axis. Due to the rotational symmetry of the Hamiltonian, any choice of \hat{e} is equivalent, and for the sake of concreteness we take $\hat{e} = \hat{z}$. The Hamiltonian has a twist-dependent ground state $|\Omega_\phi\rangle$, allowing to define the following geometric

phase as the topological invariant

$$\Phi_{\text{spin}} = i \int_{\phi=0}^{2\pi} \langle \Omega_{\phi} | \partial_{\phi} | \Omega_{\phi} \rangle d\phi. \quad (\text{S11})$$

The geometric phase takes a value of $\pm\pi$ for $J_K > 0$, demonstrating the topological origin of the zero modes.